Int. J. Electrochem. Sci., 13 **(2018)** 5956 – 5962, doi: 10.20964/2018.06.68

International Journal of
ELECTROCHEMICAL
SCIENCE
www.electrochemsci.org

Short Communication

Synthesis and Electrochemical Properties of Spinel-type $Li_4Mn_{5-x}Ti_xO_{12}$ Materials

Xin Wu, Min Zeng[*]*, Lige Wang, Jin Li*

School of Materials Science and Engineering, Southwest University of Science and Technology,
Mianyang 621010, P R China
[*]E-mail: zengmin@swust.edu.cn

Received: 21 February 2018 / *Accepted:* 11 April 2018 / *Published:* 10 May 2018

Cathode materials and anode materials are the focus of current research in lithium ions battery. In this study, $Li_4Mn_{5-x}Ti_xO_{12}$ (x=0-5) powders were prepared by a solid-state method, which calcined from 600°C to 800°C for 10 h. The chemical and physical properties of as-prepared powders had been characterized by XRD and SEM, and shown that the crystal phases of the powders crystallized to the spinel-type structure (Fd-3m). The discharge capacity and cycling performance of Ti-doped $Li_4Mn_{4.9}Ti_{0.1}O_{12}$ cathode material and of Mn-doped $Li_4 Ti_{4.95}Mn_{0.05}O_{12}$ anode material had improved, from the electrochemical measurement. The reason may be due to the metal ions substitution help to stabilize the crystal structure during electrochemical insertion/extraction of Li^+. We also discovered that $Li_4Mn_{2.5}Ti_{2.5}O_{12}$ material was not suitable as anode materials, but still suitable as cathode materials for lithium battery, although its discharge capacity very low.

Keywords: Li-ion batteries, $Li_4Mn_{5-x}Ti_xO_{12}$, anode material, cathode material, electrochemical propertie.

1. INTRODUCTION

Lithium-ion batteries (LIBs) have been extensively applied to portable electronic devices and also hybrid vehicles due to their high power and energy densities [1]. And the most successful commercial anode material graphite and cathode material $LiCoO_2$ have a relatively low actual capacity, and could not meet the tremendous needs of the high-energy applications [1].Therefore, it is very important to synthesis and studies the high performance electrode materials, which determine the potential window, rate capability, energy density and cycling stability [1-2]. On the other hand, Spinel-type transition metal oxides have been always considered as important electrode materials of lithium extraction–insertion reactions [2]. As in $Li_4Mn_5O_{12}$ and $Li_4Ti_5O_{12}$, spinel-type oxides containing tetravalent Ti and Mn have very interesting properties. Layered-spinel $Li_4Mn_5O_{12}$ is a cathode material with a theoretical capacities of 163 mAh·g^{-1}, and spinel-type $Li_4Ti_5O_{12}$, with a theoretical capacities of 175 mAh·g^{-1}, has been considered as a good anode material for LIBs [3-4]. There difference in electrochemical performances, although its structure is extremely similar, should be due to the chemical valence for Ti involving the +3/+4 redox couples, but for Mn involving the +5/+4 [3-4]. $Li_4Mn_5O_{12}$ material, also represented as $Li_{4/3}Mn_{5/3}O_4$, has great advantage such as economic flexibility, non-toxicity, environmentally friendliness and able to provide high cell voltage, and large operating temperature range. However, their electrochemical performances are still unsatisfactory because of the difficulties in preparation Mn^{4+} [3]. On the other hand, $Li_4Ti_5O_{12}$ anode materials, despite several advantages remain such as outstanding safety performance and ultra-long lifetime also has some drawbacks such as poor electronic conductivity and slow Li-ion transfer in the bulk material [4].

To overcome these drawbacks, a variety of strategies have been developed, ranging from cation doping and synthesize a lithium additional materials to approaches including coating and nanosizing [4-7]. It was reported that metal ions substitution (e.g., Mg, La, Sb, Cr, Ni, Fe) of Ti for $Li_4Ti_5O_{12}$ anode material were found to be a highly promising approach, in increase the capacity, rate capability as well as capacity retention [7-15]. Among these metal-doping, Mn is one of the most attractive candidates, due to its variable oxidation states, cost effectiveness as well as environmentally compatibility [16-17]. Oddly enough, there are very limited reports in the literature on mixed spinels containing both Mn^{4+} and Ti^{4+}, especially for the Ti doping $Li_4Mn_{5-x}Ti_xO_{12}$ cathode [17]. We have discovered that because both $Li_4Mn_5O_{12}$ and $Li_4Ti_5O_{12}$ are the same structure, the spinel-type $Li_4Mn_{5-x}Ti_xO_{12}$ (x=0-5) is easy to obtained [18-19]. When Ti dope to $Li_4Mn_5O_{12}$, because the redox reactions both Mn and Ti occurred in lithium ion battery with the operating voltage of 3V the higher rechargeable capacity of spinel-type $Li_4Mn_{5-x}Ti_xO_{12}$ is expected [20]. In this work, $Li_4Mn_{5-x}Ti_xO_{12}$ (x=0-5) powders were prepared by a solid-state method, which calcined from 600°C to 800°C for 10 h. The powder characteristics of $Li_4Mn_{5-x}Ti_xO_{12}$, the effects on the electrochemical property of Ti-doping $Li_4Mn_{5-x}Ti_xO_{12}$ cathode and of Mn-doping $Li_4Mn_{5-x}Ti_xO_{12}$ anode were investigated.

2. EXPERIMENTAL

2.1. Synthesis of $Li_4Mn_{5-x}Ti_xO_{12}$ materials

Ti-doped $Li_4Mn_{5-x}Ti_xO_{12}$ (x=0-2.5) cathode materials were synthesized by the traditional solid-state method [8]. At first, Li_2CO_3, MnO_2 and TiO_2 were mixed according to the molar ratio and milled homogeneously in an agate mortar. And the mixtures were calcined in air from 20°C to 600°C at a heating rate of 5°C min^{-1} and then kept at 600°C for 10h for x=0-0.1 samples [3], but for x=0.1-2.5, which annealed at 800 °C for 10 h [18-19], respectively. Subsequently, the resultant product must be milled again to adjust the grain size of the coarse particles caused by high temperature calcinations. Similarly, Mn-doped $Li_4Mn_{5-x}Ti_xO_{12}$ (x=2.5-5.0) anode materials also were synthesized that annealed at 800 °C for 10 h [18-19]. X-ray diffraction (XRD) patterns were obtained on an X'Pert PRO (PAN analytical) with a Cu Ka radiation at a range of 10-80°. The morphologies and microstructures of the samples were observed by a Fieldemission scanning electron microscopy (FESEM, Zeiss Ultra 55).

2.2. Electrochemical Measurements

For electrochemical evaluation, the working electrodes were made by mixed the active material, super-P and polyvinylidene difluoride (PVDF) in a weight ratio of 8:1:1. The mixture was dissolved in N-methylpyrrolidone (NMP) solvent to form homogeneous slurry, milled and plastered onto a Cu foil, then dried at 120 ℃ for 24 h. Subsequently, these electrodes were cut into discs about 1mg cm^{-2} and assembled into CR2016 coin half cells in an Ar-filled glove box with Li foil as the negative electrodes and polypropylene microporous film (Celgard 2300) as the separators [10]. The electrolyte was 1M $LiPF_6$ dissolved in ethylene carbonate (EC), diethyl carbonate (DEC) with a ratio of 1:1. Before testing, these assembled cells were grounded for 12 h at room temperature. Galvan static charge-discharge measurements were investigated using a LAND test systems over a voltage window of 1.0-4.5V (vs. Li^+/Li).

3. RESULTS AND DISCUSSION

3.1 Powder characteristics

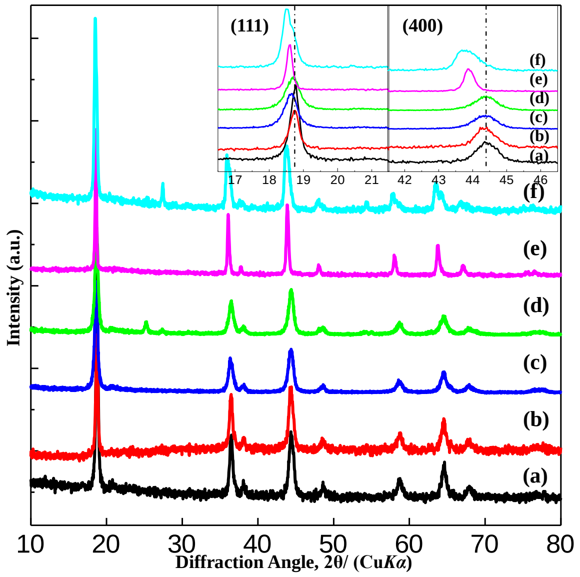

Figure 1. XRD patterns of Ti-doped $Li_4Mn_{5-x}Ti_xO_{12}$ cathode material: (a) x=0, (b) x=0.05, (c) x=0.1, which annealed at 600 °C for 10 h; (d) x=1, (e) x=2, (f) x=2.5, which annealed at 800 °C for 10 h, respectively.

The chemical composition and crystal phases of the obtained powders were investigated by using the XRD. As shown in Fig. 1, the characteristic diffraction peaks of the Ti-doped $Li_4Mn_{5-x}Ti_xO_{12}$ (x=0-2.5) samples correspond to the planes of well-crystallized spinel structure, which fits well to the space group of Fd-3m, consistent with previously reported data [3, 18, 21]. The results also shown that, because the radius of Ti^{4+} (0.605 Å) is larger than that of Mn^{4+} (0.53Å), the diffraction angle in the (111) and (400) planes decreased with the Ti content increased. Fig. 2 shown the XRD patterns of Mn-doped $Li_4Mn_{5-x}Ti_xO_{12}$ (x=2.5-5) anode material, which annealed at 800 °C for 10 h. The characteristic diffraction peaks of the samples also were in good agreement with the spinel structure, and the diffraction angle in the (111) and (400) planes increased with the Mn content increased [18]. Thus, it is reasonable to suggest that the Ti^{4+} ions disperse into the $Li_4Mn_5O_{12}$ lattice, and this solid-state method for preparation of the $Li_4Mn_{5-x}Ti_xO_{12}$ spinel materials is reliable [18-19].

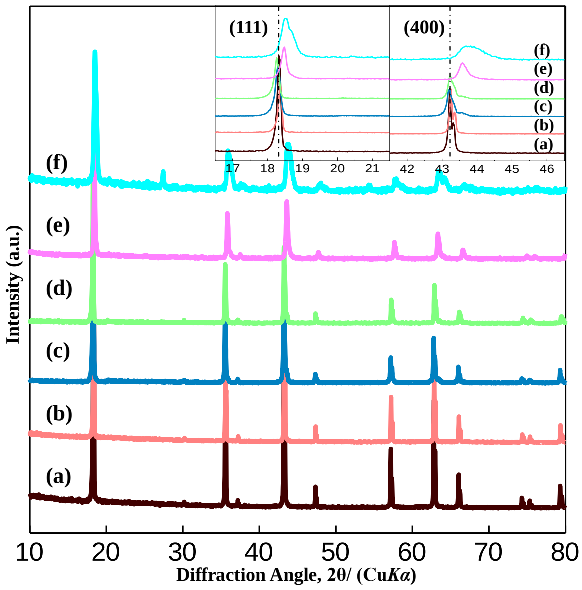

Figure 2. XRD patterns of Mn-doped $Li_4Mn_{5-x}Ti_xO_{12}$ anode material, which annealed at 800 °C for 10 h: (a) x=5, (b) x=4.95, (c) x=4.9, (d) x=4, (e) x=3, (f) x=2.5, respectively.

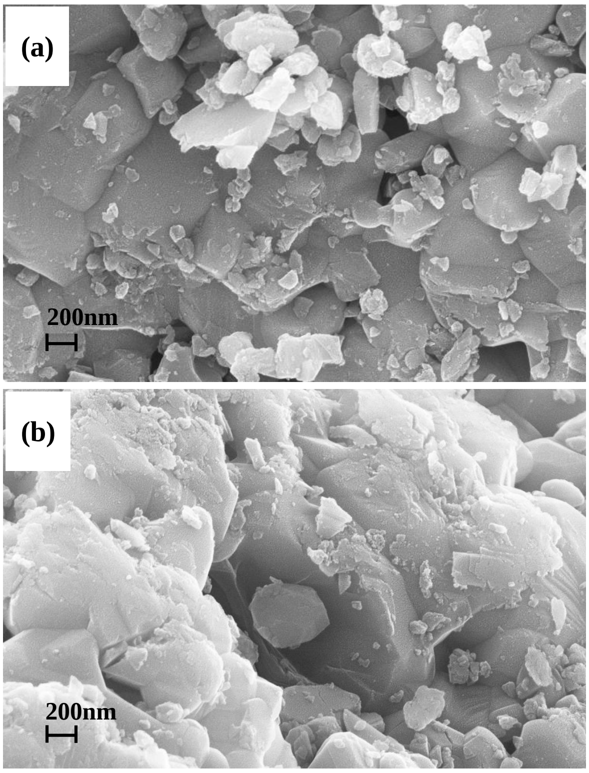

Figure 3. SEM images of (a) $Li_4Mn_5O_{12}$ which annealed at 600 °C for 10 h and (b) $Li_4Ti_5O_{12}$ which annealed at 800 °C for 10 h.

The morphology and structure of $Li_4Mn_5O_{12}$ which annealed at 600 °C for 10 h and $Li_4Ti_5O_{12}$ which annealed at 800 °C for 10 h were illustrated by field emission scanning electron microscopy (FESEM), as shown in Fig. 3. From the FESEM picture, it can be found that the solid-state sintered materials are agglomerated with no fixed morphology, although the particle size of $Li_4Mn_5O_{12}$ was looked like smaller than that of $Li_4Ti_5O_{12}$.

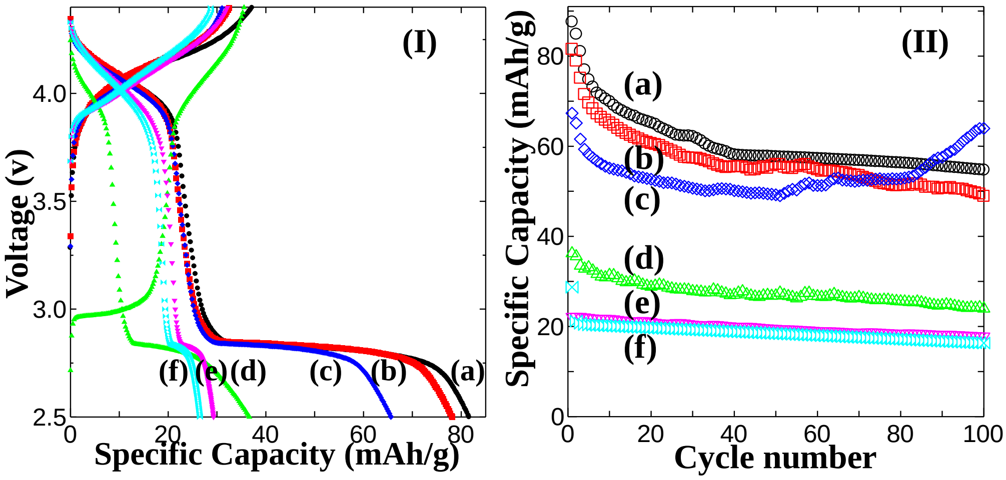

Figure 4. Galvanostatic charge/discharge curves (I) and cyclic performance at a rate of 1 C (II) of Ti-doped $Li_4Mn_{5-x}Ti_xO_{12}$ cathode material: (a) x=0, (b) x=0.05, (c) x=0.1, (d) x=1, (e) x=2, (f) x=2.5, respectively.

3.2 Electrochemical properties

The electrochemical performance of the Ti-doped $Li_4Mn_{5-x}Ti_xO_{12}$ (x=0-2.5) samples as cathode materials for LIBs was evaluated. Fig. 4 show the Galvanostatic charge/discharge curves (I) and cyclic performance at a rate of 1 C (II) in the voltage range 2.5-4.5 V (vs. Li/Li+). As shown in Fig. 4 (I), the voltage profiles present two obvious long plateaus at 4.02 and 2.85 V respectively, exhibiting the typical characteristics of $Li_4Mn_5O_{12}$ cathode materials [3, 21]. The initial discharge capacity values of $Li_4Mn_{5-x}Ti_xO_{12}$ (x=0-2.5) were 82 $mAh{\cdot}g^{-1}$, 78 $mAh{\cdot}g^{-1}$, 65 $mAh{\cdot}g^{-1}$, 37 $mAh{\cdot}g^{-1}$, 30 $mAh{\cdot}g^{-1}$ and 27 $mAh{\cdot}g^{-1}$ respectively. With the titanium content increases, the battery capacity decreases significantly. As shown in Fig. 4 (II), the capacity fading of $Li_4Mn_5O_{12}$ is about 31 %. The reason may be due to the Jahn-Teller effect which reduces the crystal symmetry of the structure to tetragonal symmetry, resulting in a degradation of the structural integrity of the electrode and loss of cycling efficiency [20]. Although the initial capacity of $Li_4Mn_{4.9}Ti_{0.1}O_{12}$ cathode materials is quite low, the capacity fading is only about 2 %. This might be due to the Ti^{4+} help to stabilize the crystal structure during electrochemical insertion/extraction of Li^+.

Fig. 5 shows the Galvanostatic charge/discharge curves (I) and cyclic performance at a rate of 1 C (II) of the Mn-doped $Li_4Mn_{5-x}Ti_xO_{12}$ (x=2.5-5) anode materials in the voltage range 3-1V (vs. Li/Li+). As shown in Fig. 5 (I), the voltage profiles present two obvious long plateaus at 1.62 and 1.55

V respectively, exhibiting the typical characteristics of $Li_4Ti_5O_{12}$ anode materials [4]. The initial charge capacity values of $Li_4Mn_{5-x}Ti_xO_{12}$ (x=2.5-5) were 201 mAh·g^{-1}, 220 mAh·g^{-1}, 107 mAh·g^{-1}, 150 mAh·g^{-1}, 45 mAh·g^{-1} and 28 mAh·g^{-1} respectively. As shown in Fig. 5 (II), the capacity fading of $Li_4Ti_5O_{12}$ is about 20 % before 30 cycles, and then the capacity tended to be stable. The capacity of $Li_4Mn_{0.05}Ti_{4.95}O_{12}$ anode materials is higher than that of $Li_4Ti_5O_{12}$, and has better cycle stability. But with the Mn content increases, the battery capacity decreases significantly. As shown in Fig. 5 (d, e, f), some strange charge/discharge curves indicated that these $Li_4Mn_{5-x}Ti_xO_{12}$ (x=4, 3, 2.5) materials are not suitable for lithium battery anode materials.

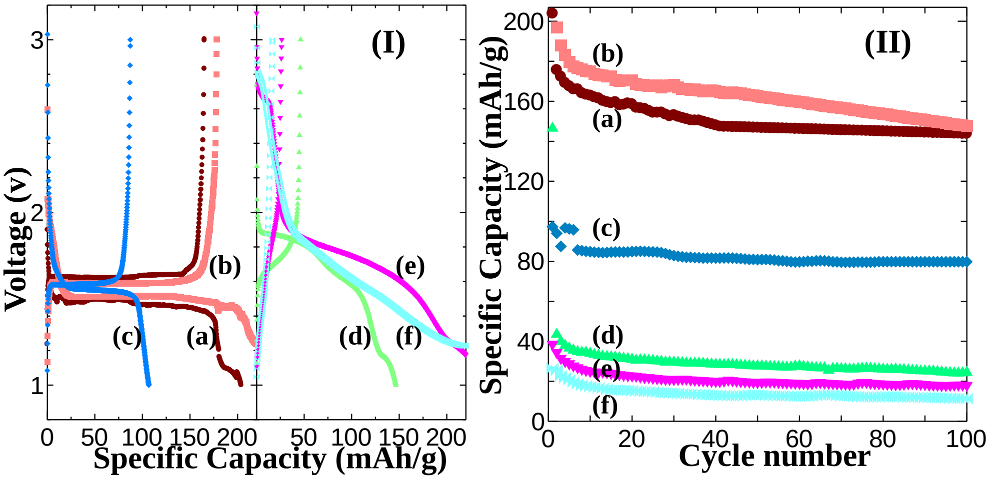

Figure 5. Galvanostatic curves (I) and cyclic performance at a rate of 1C (II) of Mn-doped $Li_4Mn_{5-x}Ti_xO_{12}$ anode material: (a) x=5, (b) x=4.95, (c) x=4.9, (d) x=4, (e) x=3, (f) x=2.5, respectively.

4. CONCLUSIONS

In summary, Ti-doped $Li_4Mn_{5-x}Ti_xO_{12}$ (x=0-2.5) cathode materials and Mn-doped $Li_4Mn_{5-x}Ti_xO_{12}$ (x=2.5-5.0) anode materials were prepared by the traditional solid-state method. XRD revealed that the homogeneous crystal phase of spinel-type $Li_4Mn_{5-x}Ti_xO_{12}$ obtained by calcining from 500 to 800°C. The electrochemical measurement showed that the cycling performance of Ti-doped $Li_4Mn_{4.9}Ti_{0.1}O_{12}$ cathode material and of Mn-doped $Li_4Mn_{0.05}Ti_{4.95}O_{12}$ (x=4.95) anode material had improved. We also discovered that $Li_4Mn_{5-x}Ti_xO_{12}$ (x=4, 3, 2.5) materials are not suitable as anode materials, and the discharge capacity of $Li_4Mn_{5-x}Ti_xO_{12}$ (x=1, 2, 2.5) cathode materials are very low.

References

1. B. Dunn, H. Kamath, J.M. Tarascon, *Science*, 334 (2011) 928.
2. D. Wang, X. Wang, R. Yu, Y. Bai, G. Wang, M. Liu, X. Yang, *Electrochim. Acta*, 190 (2016) 1142.
3. Sv. Ivanova, E. Zhecheva, D. Nihtianova, R. Stoyanova, *J. Mater. Sci.*, 46 (2011) 7098.
4. L. Shen, X. Zhang, E. Uchaker, C. Yuan, G. Cao, *Adv. Enengy Mater.*, 2(2012) 691.
5. L. Yu, H. Wu, X. Wen, D. Lou, *Adv. Mater.*, 25(2013) 2296.
6. L. Wang, Y. Zhang, M. E. Scofield, S. Yue, C.y McBean, A. C. Marschilok, K. J. Takeuchi, *ChemSusChem*, 8(2015) 3304.

7. W. Wang, B. Jiang, W. Xiong, Z. Wang, S. Jiao, *Electrochim. Acta*, 114(2013) 198.
8. F. Li, M. Zeng, J. Li, H. Xu, *Int. J. Electrochem. Sci.*, 10(2015) 10445.
9. Y. Bai, C. Gong, Y. Qi, N. Lun, J. Feng, *J. Mater. Chem.*, 22(2012) 19054.
10. F. Li, M. Zeng, J. Li, X. Tong, H. Xu, *RSC Adv.*, 6(2016) 26902.
11. M. Ganesan, *Ionics*, 14(2008) 395.
12. L. G. Wang, F. Y. Li and M. Zeng, *Int. J. Electrochem. Sci.*, 11 (2016) 9941.
13. Y. Ma, B. Ding, G. Ji, J. Y. Lee, *ACS Nano*, 7(2013) 10870.
14. K. Ding, Y. Zhao, M. Zhao, Y. Li, J. Zhao, Y. Chen, Q. Wang, *Int. J. Electrochem. Sci.*, 10(2015) 7917.
15. Z. Xie, H. Eikhuemelo, J. Zhao, C. Cain, W. Xu, Y. Wang, *J. Electrochem. Soc.*, 162(2015) 1523
16. D. Capsoni, M. Bini, V. Massarotti, P. Mustarelli, G. Chiodelli, C. B. Azzoni, M. C. Mozzati, L. Linati, S. Ferrari, *Chem. Mater.*, *20* (2008) 4291.
17. H. Kaftelen, M. Tuncer, S. Tu, S. Repp, H. Gocmez, R. Thomann, S. Weber, E. Erdem, *J. Mater. Chem. A*, 1(2013) 9973.
18. V.D. Nithya, R. K. Selvan, K. Vediappan, S. Sharmila, C. W. Lee, *Appl. Surf. Sci.*, 261 (2012) 515.
19. T. Omura, T. Kodera, T. Ogihara, *J. Ceram. Soc. Japan*, 123(2015) 280.
20. M. Le, P. Strobel, C. V. Colin, *J. Phys. Chem. Solids*, 72 (2011) 124.
21. N. H. Zainol, Z. Osman, N. Kamarulzaman, R. Rusdi, *Ionics*, 23 (2017) 303.